Monthly and Annual Phase Delay Statistics Acquired from DSN and KSC Site Test Interferometers

David D. Morabito*

ABSTRACT. — Site Test Interferometers (STI) have been operating at the three Deep Space Network (DSN) tracking sites and Kennedy Space Center (KSC) to gather statistical data on spatial phase fluctuations induced by the atmosphere. Such data is useful for characterizing the suitability of each site to host potential antenna uplink arrays at high frequency bands (e.g., Ka-band) for telecommunications and navigation applications. As part of the effort, the phase delay statistics are characterized on a monthly and annual basis. Eight full years of data for Goldstone Apollo (2011–2018) were acquired, seven years for Canberra (2012–2018) (with some partial months in 2011), five full years for Madrid (2014–2018), and five years at KSC (2014–2018). Thus, phase delay statistics were derived from STI data spanning 2011 to 2018.

I. Introduction

Until recently, space communications have relied primarily on lower frequency bands such as S-band (2.3 GHz) and X-band (8.4 GHz). However, these frequency bands are limited in bandwidth and thus limited in data rate. Given the desire and necessity to transition to higher data rates, higher frequency bands are being used more and more for downlink. These bands include the deep-space Ka-band (32 GHz) and near-Earth K-band (26 GHz). However, these higher frequency bands are more susceptible to degradation due to atmospheric effects. Given that NASA will be required to provide services using high availabilities (such as at 99%) using Gb/s data rates (versus current ~ Mb/s data rates), the atmospheric phase stability (time delay fluctuations) and atmospheric attenuation of candidate sites are required to be well-characterized [1]. One can use Site Test Interferometers (STI) that continuously measure the difference in signal delay from a celestial source (typically a geostationary satellite) to two or more points on the Earth [1]. The resulting variations in the delay differences are principally due to atmospheric turbulence, mostly due to water vapor [2]. The received signal phase difference is measured on short ~1 s time scales. During post-processing, long-period trends due to satellite motion and instrumental drift are removed. Fluctuations in the resulting phase delay

* Communications Architectures and Research Section.

The research described in this publication was carried out by the Jet Propulsion Laboratory, California Institute of Technology, under a contract with the National Aeronautics and Space Administration. © 2019 California Institute of Technology. U.S. Government sponsorship acknowledged.

residuals are dominated by the troposphere on timescales ranging from sub-second to several hundred seconds. The phase delay statistics vary between sites due to climate, weather conditions, terrain, and altitude. These statistics also vary at any one site diurnally, seasonally, and with passage of weather systems. The observed turbulence varies with weather and season, but its effect over ~200 m distance scales is not measurable by ordinary meteorological instruments, hence the need for this specialized instrument. The STI provides a long-term statistical characterization of a site. The resulting statistics on phase delay will also help potential or present downlink arrays determine how much of their signal energy is being or will be disrupted by the atmosphere in real-time, and thus provide a measure of how well any atmospheric compensation process is working.

Given that an STI and a nearby communication antenna array experience the same short- and long-term statistical delay fluctuations, the instantaneous delay as measured by the STI is generally not useful for real-time correction of delay errors in an uplink array.[1] This is because their signal targets usually lie in different locations in the sky and thus their signals pass through different parts of the turbulent media. However, statistics acquired over multi-year periods are useful for site characterization. One can employ these long-term statistics to determine the suitability of a site for hosting an array or use them in communication link budgets for current or proposed missions using an array. Operating these STIs over long periods allows for acquisition of sufficient data to provide for reliable site characterization. The phase fluctuations have dependency with site location and vary with weather conditions and array configuration. Thus, their statistics are useful for determining site suitability and the maximum size of an array that can operate efficiently at a given site and frequency [3].

II. Previous Work

Several STI instruments were built at the Jet Propulsion Laboratory in Pasadena, California, and are based on a design provided by the Harvard Smithsonian Center for Astrophysics (CfA). Nearly identical instruments involving three baselines were deployed in the Apollo Valley at Goldstone, California; at Canberra, Australia; at Madrid, Spain, and at Kennedy Space Center (KSC). In addition, two-element versions of this design were deployed in South Africa and West Australia to support radio astronomy activities. Other STIs have been operating at various radio astronomy sites for numerous years. The KSC STI was deployed at the site of a preliminary array demonstration involving three 12-m diameter antennas for a project known as KaBOOM [1, 4].

An STI of a different design in collaboration with the NASA Glenn Research Center (GRC) was deployed in May 2007 at Goldstone at the Venus antenna site where the R&D 34-m antenna DSS-13 resides. This two-element instrument consisted of 1.2-m diameter antennas forming an interferometer of 256 m separation oriented in the east–west direction. This STI operated at 20.2 GHz and continuously observed the ANIK F2 satellite at an elevation of 48.5° for several years. Details of the operation of this STI are discussed elsewhere [5–7], including discussion on data processing [8] and early phase fluctuation

[1] For a downlink array, the array processor can calibrate atmospheric phase fluctuations making use of a strong reference carrier using appropriate algorithms. For uplink arrays, such compensation is not normally feasible, so the site characterization described here is more important for that case.

results [9]. The slope of the temporal structure function of the phase delay (prior to the knee) with time interval, τ, agreed very well with the thick layer model slope $\tau^{5/3}$ during the hottest summer day, and with the thin layer model slope $\tau^{2/3}$ during the coldest winter night at Goldstone, in agreement with the Kolmogorov model [10]. Most of the time, the resulting slope fell between these two limits. Uplink array loss was presented for sample antenna array configurations as a function of frequency and RMS delay fluctuation [10].

Data from two independent instruments occupying the same complex, Goldstone Apollo and the Goldstone Venus STIs, were utilized in an inter-comparison study [11–12]. Both instruments were deployed to assess the suitability of Goldstone for uplink arraying and to statistically characterize the atmosphere-induced phase variations for application to future arrays. The GRC Venus STI data and the Apollo STI data (using the east-west baselines) were examined temporally and statistically. Both instruments consist of two ~1 m diameter antennas and associated electronics separated by ~200 m. The two Goldstone STI locations were separated by 12.5 km and have an elevation difference of 119 m. It was found that the delay fluctuations between the two sites were statistically similar and did not appear to be shifted versions of each other, suggesting that the length scale for evolution of the turbulence pattern is shorter than the separation between instruments. Another significant result was that the fluctuations were slightly weaker at the higher altitude site but consistent with theory [11–12].

The Venus STI was also involved in a comparison study involving similar data extracted from Water Vapor Radiometer (WVR) sky brightness measurements. In August 2008, two WVR units were deployed next to each STI element in an attempt to provide ancillary data that can be used in an inter-comparison with the STI phase fluctuations. The sky brightness temperature measurements acquired at different sky frequencies from the WVRs were converted to path delays, which were then differenced between the two WVRs. This difference data type was then compared with the concurrent STI path delay for the month of August 2008. The inter-comparison study showed that the temporal behavior and the statistics of the two data types were consistent and in reasonable agreement after making the appropriate adjustments [13].

A study involving a comparison between concurrent STI data and arrayed signal data at Ka-band received at two DSN antennas within the same complex was also conducted. This study was motivated by NASA's interest in using the technique of arraying smaller diameter antennas to increase effective aperture to replace the aging 70-m monolithic structures of the DSN. Downlink arraying is routinely performed by the DSN at 8.4 GHz (X-band) for certain missions. This technique is expected to be extended to uplink arraying. The received signals from two individual DSN antennas were recorded and processed to obtain independent estimates of interferometer phase to be compared against STI phase after making appropriate adjustments for frequency, elevation angle, and baseline length [14].

The fades predicted from the difference of the individual station DSS-25 and DSS-26 received phases of the Cassini spacecraft Ka-band signal using open-loop receiver recordings (processed and adjusted, etc.) were found to be in good agreement with measured fades from array processing equipment [14–15], providing confidence that the

two instruments were measuring the same quantity. The amplitude fades estimated from the array processor data were of roughly comparable magnitude as those estimated from the adjusted STI phase data, but their phase time series were not expected to agree since the STI and DSN array were pointed in different directions in the sky. However, the statistics of the STI fade magnitude range were comparable to that of the DSN array. That is, the distribution of the array phase difference estimates extracted from the individual antenna data was found to be statistically similar to that of the STI phase data (after appropriate adjustments were applied for sky frequency, baseline length, and elevation angle). The individual time series of the two sets of phase fluctuations revealed many features that were correlated, anti-correlated, and time delayed, suggesting the presence of differences in dynamic atmospheric features as the signals propagated across similar and different atmospheric cells.

Recent Kepler spacecraft Ka-band arrayed data over a much longer ~12.5 km baseline using DSS-25 and another more distant 34-m diameter antenna at Goldstone (DSS-13) validated the thin screen turbulence model [15]. The DSN array and STI results of several additional demonstrations were found to be similar [15].

Finally, the significance of the phase delay statistics presented in this paper can be related to the feasibility of conducting uplink arraying operations by examining derived array loss statistics. For downlink arraying, atmospheric phase effects can be removed via processing when there is sufficient strength in the received signal serving as a reference. However, in the absence of a reference signal such as for uplink arraying, or a weak reference signal for downlink arraying, one needs to rely on factoring in atmospheric array loss in any link predictions. In a previous study, monthly and annual phase delay statistics were adjusted by element separation, elevation angle and frequency to yield estimates of array loss for different combinations of 34-m diameter antennas (2-element and 3-element) at Goldstone and Canberra [16]. These estimates were presented in tables as a function of availability for both monthly and annual cases for these two sites. The Madrid results were expected to be similar to those of Canberra. At the X-band uplink frequency of 7.15 GHz, it was found that the array loss at ~99% and 20 deg elevation ran ~0.6 dB for Goldstone and ~1.4 dB for Canberra, making X-band viable for uplink arraying at these two sites. At the Ka-band uplink frequency of 34.5 GHz, it was found that the array loss at ~99% and 20 deg elevation ran ~3 dB or above for both Goldstone and Canberra. Thus, with array loss at 3 dB or higher, one would just revert to using one antenna for uplink. Thus, Ka-band would not be viable for uplink arraying at either Goldstone or Canberra except at the lowest availabilities.

III. Site Characteristics

A general description of the STIs were previously provided in Section II. The photos in Figure 1 provide examples of each site's terrain along with one of the antenna/electronics box elements. Table 1 specifies key details of each of the STI instruments.

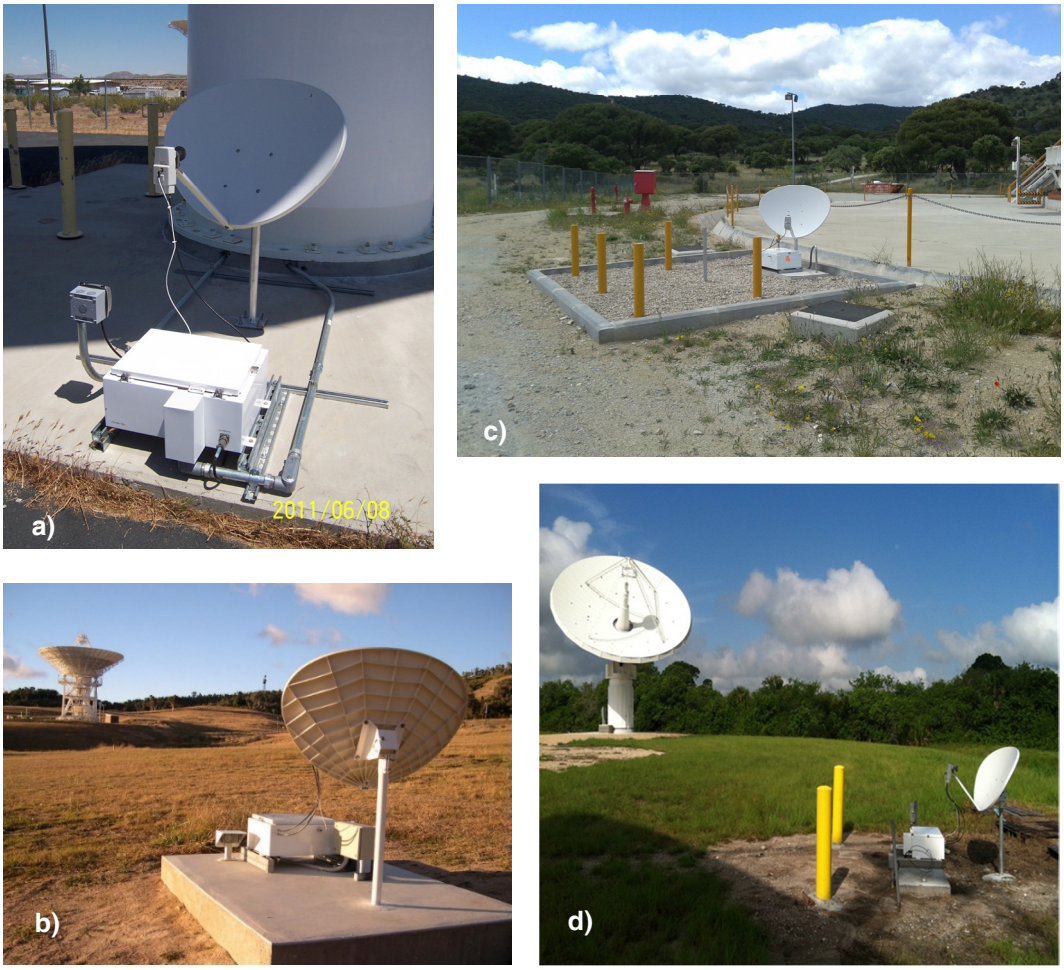

Figure 1. Photos of STI elements at the four sites: a) STI element at Apollo site in Goldstone, California; b) STI element in Canberra Australia; c) STI element at Madrid, Spain; and d) STI element (foreground) at KSC, Florida, along with one of the larger antennas of the KaBOOM demonstration (background).

The KSC STI uses three small (0.8 m) antennas in a triangular configuration with varying spacing of the baselines from 135 to 289 m to receive and process signals from a commercial geostationary satellite. In contrast, the Canberra STI has nearly identical spacing of its three baselines about 200-m each. Although each of the four sites involve three baselines, the phase delay statistics itemized in this report are from only one baseline whose lengths are noted in Table 1.

Phase delay statistics were normalized to a common elevation angle (zenith) using the appropriate adjustment formulation [16–19] to facilitate inter-comparison between sites (such as shown in Figures 2–5). For the periodic delivery of these statistics to International Telecommunications Union (ITU) databanks [20], only adjustments in frequency (from the measured phase at different frequencies to delay) were performed (such as shown in Figures 6–7). Thus, the resulting statistics in Figures 6–7 are referenced to line-of-sight (LOS). The databank submissions are accompanied by a document that provides background information and discusses the data processing techniques for the application of atmospheric-induced path-length statistics that are provided in Recommendation ITU-R

P.311 Databanks [21]. This fascicle provides for information on how to convert the line-of-sight statistics to other elevation angles, element separations, and frequencies for use in array link budgets.

Table 1. Summary of experiment parameters at each measurement site.

Parameter	Goldstone, CA	Canberra, AUST	Madrid, Spain	KSC Florida
Latitude	35.340 N	35.2 S	40.24 N	28.51 N
Longitude	243.126 E	148.98 E	355.75 E	279.37 E
Altitude	964 m	690 m	830 m	3 m
Baseline Separation(s)	190 m	250 m	246 m	191 m
Elevation Angle	47.1°	48.2°	41.3°	55.6°
Frequency	12.45 GHz	11.95 GHz	11.95 GHz	12.45 GHz
Satellite	CIEL 2	OPTUS D3	EUTELSAT 9A	NIMIQ 5
Orbital Position	–129° E	156.1° E	9.0° E	287.3° E

IV. Results

The temporal behavior of the phase delay RMS (in 600 s blocks, each based on 6000 samples of 0.1 s each) is presented here for each of the four sites for sample winter and summer months. The phase delay RMS was adjusted in elevation angle to reference the data to zenith, which is in units of ps.

From Figure 2, it can be seen that for the desert climate of Goldstone, the phase delay scatter is typically quiet during the cold winter months (Figure 2a), and more variable during the summer months when it is warmer and the climate is more turbulent (Figure 2b). Here the diurnal (day/night) signature stands out more clearly during the summer where the peaks occur near local noon (hotter temperature and atmosphere retains more water vapor), whereas during the winter, one could go on for several days without significant variation.

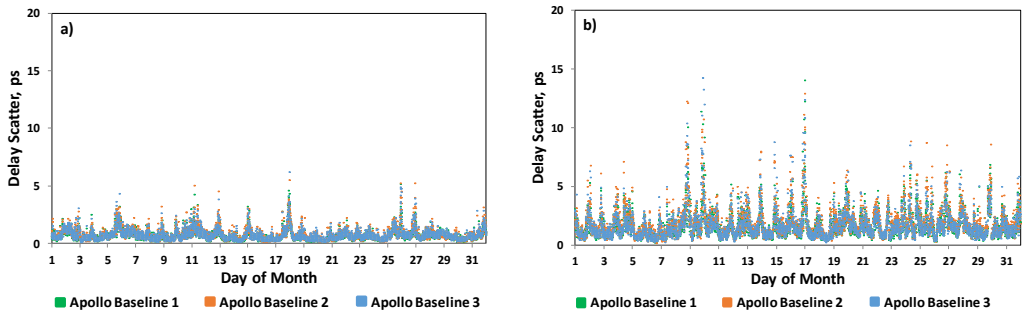

Figure 2. Examples of time series of delay scatter in 600 s intervals for all three Goldstone Apollo baselines, referenced to zenith: a) Sample winter month of December 2018, b) Sample summer month of August 2018.

From Figure 3, it can be seen that for the more temperate climate of Canberra, Australia, the phase delay scatter is not as contrasting between the seasons as it is for Goldstone (Figure 2). One can see significant day/night variation during the southern hemisphere summer (Figure 3a), but with some differences during southern hemisphere winter

(Figure 3b) where some features are extended over a few days. The diurnal (day/night) signatures stand out more clearly during the summer, whereas during the winter extended features may indicate stormy conditions, with the day/night variation not as evident during other periods.

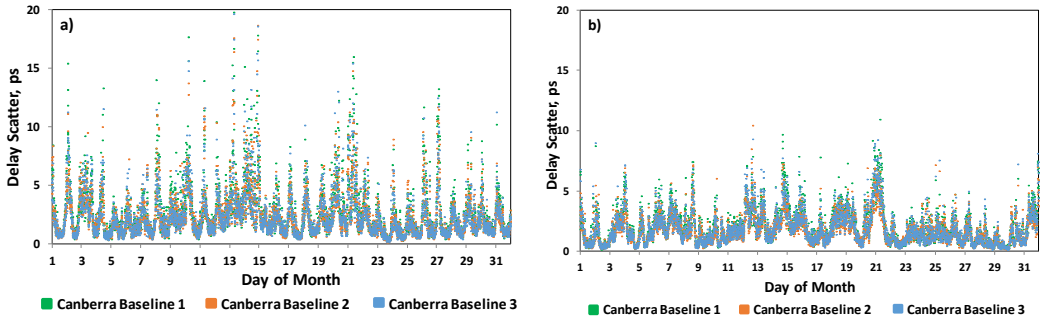

Figure 3. Examples of time series of delay scatter in 600 s intervals for all three Canberra baselines, referenced to zenith: a) Sample summer month of December 2018, b) Sample winter month of August 2018.

From Figure 4, one can see that for the temperate climate of Madrid, the phase delay scatter is typically quiet during the cold winter months (Figure 4a), with generally a little more variation when compared with Goldstone (Figure 2a). The phase delay scatter is more variable during the summer months when it is warmer and the climate is more turbulent (Figure 4b), similar to what is seen at Goldstone. Note also that the diurnal (day/night) signature stands out more clearly during the summer, whereas during the winter, one could go for several days without much discernible variation.

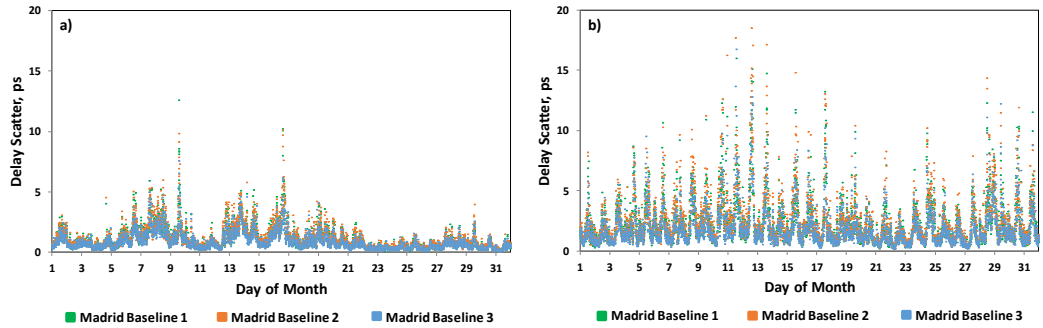

Figure 4. Examples of time series of delay scatter in 600 s intervals for all three Madrid baselines, referenced to zenith: a) Sample winter month of December 2018, b) Sample summer month of August 2018.

For the more subtropical climate of KSC, Florida, the difference of phase delay (Figures 5a and 5b) between seasons is not as extreme as the case for Goldstone (see Figures 2a and 2b). The signature of diurnal variation in phase delay RMS is more pronounced during summer (Figure 5b), and less pronounced during winter (Figure 5a), but noisier than for other sites.

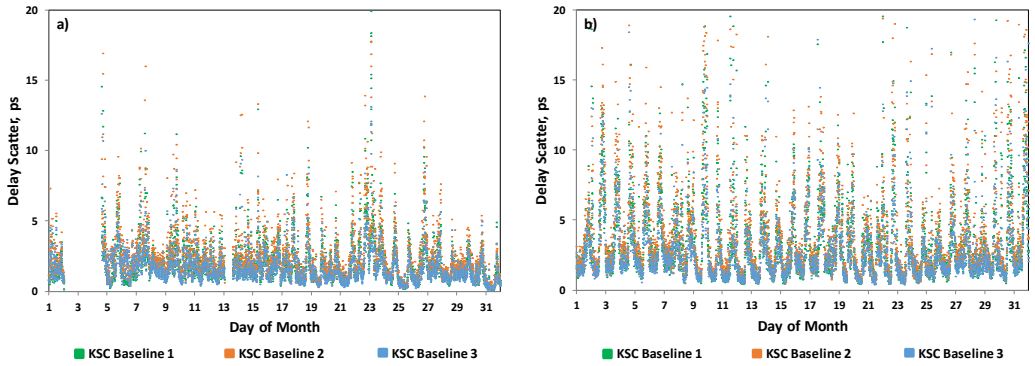

Figure 5. Examples of time series of delay scatter in 600 s intervals for all three Kennedy Space Center baselines, referenced to zenith: a) Sample winter month of January 2017, b) Sample summer month of August 2018.

The composite monthly and annual path length exceedance statistics are presented in Figures 6 and 7, respectively. The path length is referred to line-of-sight and its units are given in mm. There is significant variation of the statistics with season, where the curves for the warmer summer months generally lie to the right, the curves for the colder months generally lie to the left, and the curves for the intermediate months (autumn and spring) generally lie in between the winter and summer curves. For the northern hemisphere sites of Goldstone, Madrid, and KSC, the warmer months are usually represented by reddish colors and for the southern hemisphere site of Canberra they are represented by bluish colors. The color schemes are reversed for the colder months. The curves for the intermediate spring and autumn months are usually denoted by yellowish, greenish, and orangish colors.

Figure 6 displays the monthly exceedance statistics of path delay RMS over 600 s intervals for each of the four sites. For Goldstone (Figure 6a), the path length RMS for 0.1% exceedance varies from about 4 mm in summer to about 1.5 mm in winter, making this southwestern desert climate by far the best site in which to conduct arraying. For Canberra (Figure 6b), the path length RMS at 0.1% exceedance varies from about 6 mm in summer to about 3.5 mm in winter. For Madrid (Figure 6c), the path length RMS at 0.1% exceedance varies from about 6 mm in summer to about 1.8 mm in winter. For the subtropical KSC site (Figure 6d), the path length RMS at 0.1% exceedance varies from about 8 mm in summer to about 4.5 mm in winter, making this the most variable of the four sites considered.

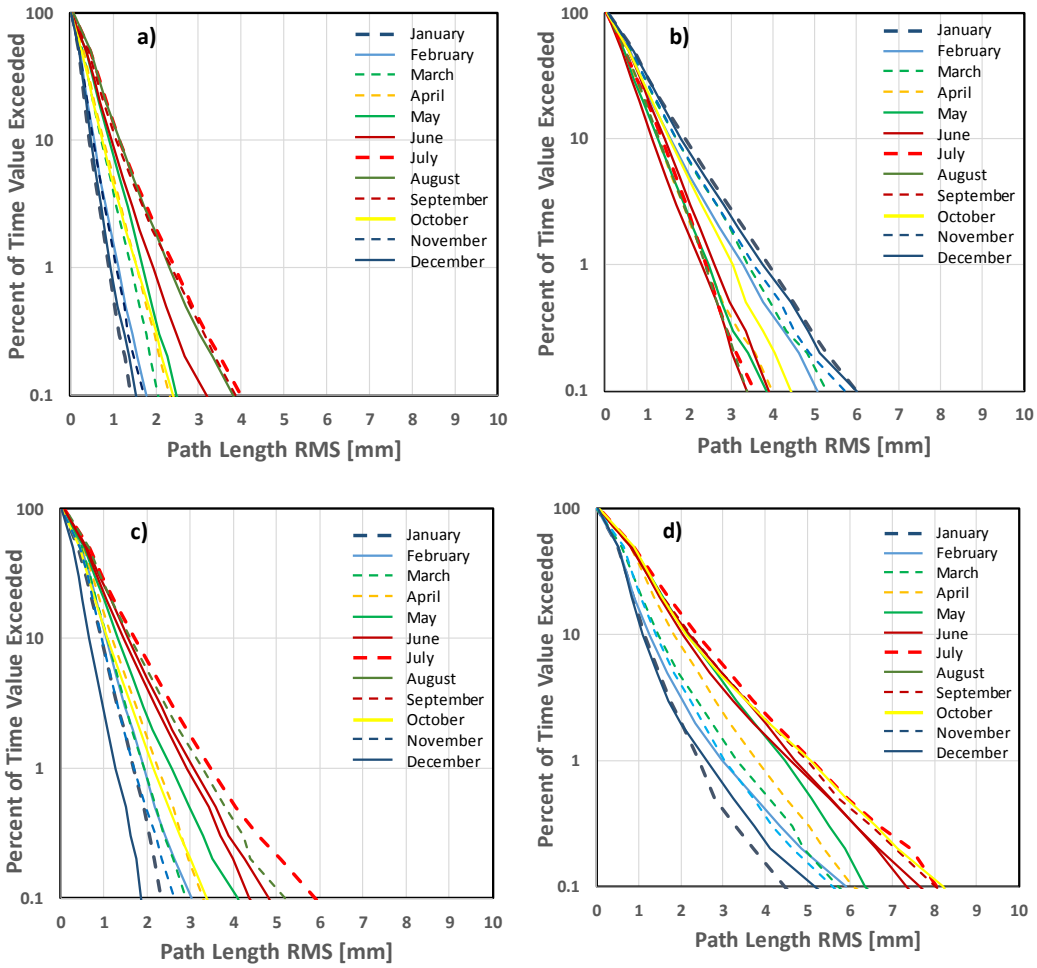

Figure 6. Path length RMS exceedance statistics for composite months, referenced to LOS: a) Goldstone, b) Canberra, c) Madrid, and d) KSC.

Figure 7 displays the annual exceedance statistics of path delay RMS over 600 s intervals for each of the four sites. For Goldstone (Figure 7a), the path length RMS for 0.01% exceedance varies from 4 to 5 mm over the different years from 2011 to 2018, making this southwestern desert climate by far the best site in which to conduct arraying. For Canberra (Figure 7b), the path length RMS at 0.01% exceedance varies from about 6 mm to about 7 mm for years 2012 to 2018. For Madrid (Figure 7c), the path length RMS at 0.01% exceedance varies from about 5.6 mm to about 6.4 mm for years spanning 2014 to 2018. For the subtropical KSC site (Figure 7d), the path length RMS at 0.01% exceedance varies from about 8.2 mm to about 9.8 mm, making this the most problematic of the four sites for arraying.

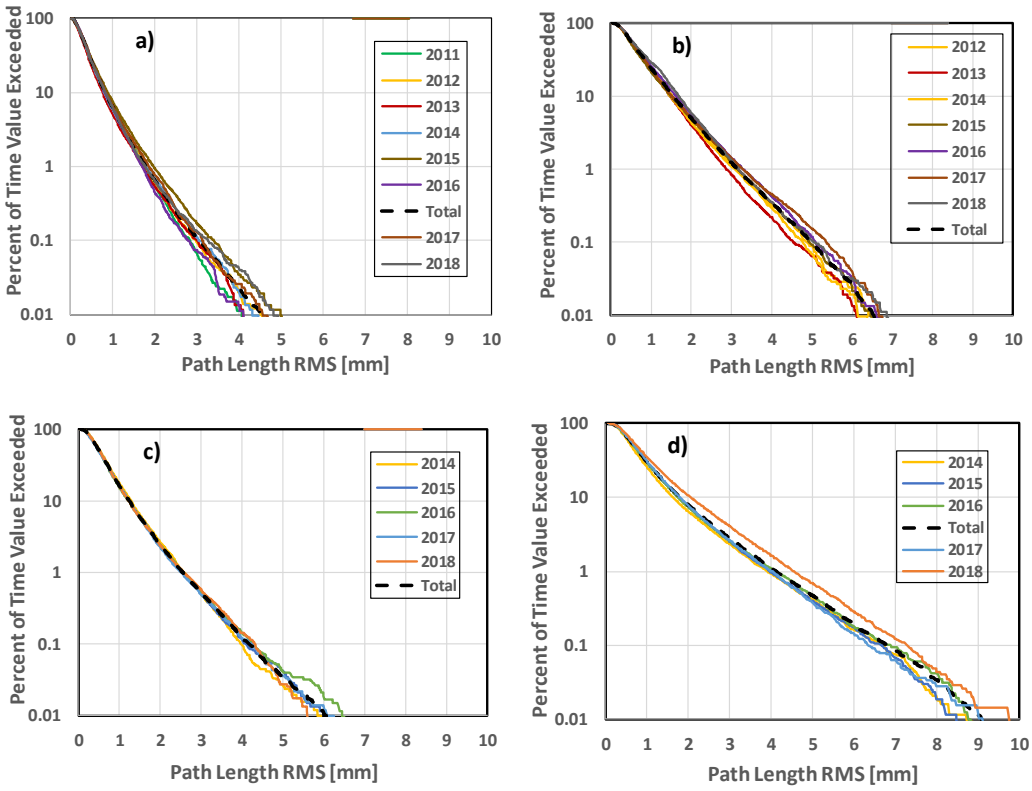

Figure 7. Annual path length RMS exceedance statistics for different years (solid colors) and for total (dashed black), referenced to LOS: a) Goldstone, b) Canberra, c) Madrid, and d) KSC.

V. Conclusion

STIs have been operating at the three DSN sites and at KSC for the purpose of gathering statistical data on spatial phase fluctuations induced by the atmosphere. These data are used to characterize the suitability of each site to host potential antenna arrays at high frequency bands (e.g., Ka-band) for telecommunications and navigation applications. The phase delay statistics were gathered from the three DSN tracking sites and the KSC site on a monthly and annual basis. The derived statistics are consistent with site climate. The dry desert climate of Goldstone, California, exhibits the lowest annual path length RMS values, and the subtropical site of KSC in Florida exhibits the highest annual path length statistics. The path length statistics for the two DSN tracking sites of Canberra, Australia, and Madrid, Spain, fall in between those of Goldstone and KSC.

Acknowledgments

The support of Faramaz Davarian of JPL and Barry Geldzahler of NASA HQ is appreciated. The support provided by the operations crews at each of the several DSN tracking sites and at KSC is also appreciated. I would also like to thank Christopher Jacobs and Victor Vilnrotter for providing valuable review comments.

References

[1] L. L. Huddleston, W. P. Roeder, D. D. Morabito, L. R. D'Addario, J. G. Morgan, R. E. Barbré, Jr., R. K. Decker, B. Geldzahler, M. A. Seibert, M. J. Miller, "Remote Sensing at the NASA Kennedy Space Center and the Eastern Range: A Perspective From the Ground Up," *Proceedings of the SPIE Remote Sensing Conference,* Amsterdam, Netherlands, September 22–25, 2014.

[2] R. N. Treuhaft and G. E. Lanyi, "The Effect of the Dynamic Wet-Troposphere on Radio Interferometric Measurements," *Radio Science,* vol. 22, no. 2, pp. 251–265, March–April 1987. doi:10.1029/RS022i002p00251. https://agupubs.onlinelibrary.wiley.com/doi/10.1029/RS022i002p00251

[3] D. D. Morabito and L. R. D'Addario, "Site Test Interferometer Atmospheric Decorrelation Statistics Use in Uplink Array Link Budgets," *Proceedings of 13th Ka and Broadband Communications Conference,* Turin, Italy, September 24–26, 2007.

[4] B. Geldzahler, M. Miller, R. Birr, K. Grant, R. Hoblitzell, L. Huddleston, J. Morgan, N. Pack, A. Sherman, G. Woods, V. Vilnrotter, T. Cornish, F. Davarian, D. Lee, D. Morabito, P. Tsao, M. Ott, H. Jakeman, W. J. Thomes, R. Switzer, J. Soloff, S. Chan, and B. Tise, "Field Demonstration of Coherent Uplink from a Phased Array of Widely Separated Antennas: Steps Toward A Verifiable Real-Time Atmospheric Phase Fluctuation Correction for a High Resolution Radar System," in AMOS Conference, Wailea, Maui, Hawaii, September 9–12, 2014. http://www.amostech.com/TechnicalPapers/2014/Orbital_Debris/GELDZAHLER.pdf

[5] R. J. Acosta, B. Frantz, J. A. Nessel, and D. D. Morabito, "Goldstone Site Test Interferometer," *Proceedings of the 13th Ka and Broadband Communications Conference,* Turin, Italy, September 24–26, 2007.

[6] J. A. Nessel, R. J. Acosta, and D. D. Morabito, "Goldstone Site Test Interferometer Phase Stability Analysis," *Proceedings of the 13th Ka and Broadband Communications Conference,* Turin, Italy, September 24–26, 2007.

[7] R. J. Acosta, J. A. Nessel, I. K. Bibyk, B. Frantz, and D. D. Morabito, "Measurements of K-Band Carrier Amplitude and Phase Fluctuations Due to Atmospheric Effects Via Interferometry," *Proceedings of the 12th Ka and Broadband Communications Conference,* Naples, Italy, September 27–29, 2006.

[8] R. J. Acosta, J. A. Nessel, and D. D. Morabito, "Data Processing for Atmospheric Phase Interferometers," *Proceedings of the 14th Ka and Broadband Communications Conference,* Matera, Italy, September 24–26, 2008.

[9] J. A. Nessel, R. J. Acosta, and D. D. Morabito, "Phase Fluctuations at Goldstone Derived From One-year Site testing Interferometer Data," *Proceedings of the 14th Ka and Broadband Communications Conference,* Matera, Italy, September 24–26, 2008.

[10] D. D. Morabito, L. R. D'Addario, S. Shambayati, R. J. Acosta, and J. A. Nessel, "Goldstone Site Test Interferometer Atmospheric Decorrelation Statistics use in Spacecraft Link Budgets: First Year of STI Data", *Proceedings of the 14th Ka and Broadband Communications Conference,* Matera, Italy, September 24–26, 2008.

[11] D. D. Morabito, L. R. D'Addario, R. J. Acosta, and J. A. Nessel, "Tropospheric delay statistics measured by two site test interferometers at Goldstone, California," *Radio Science,* vol. 48, no. 6, pp. 729–738, November/December 2013. doi:10.1002/2013RS005268. https://agupubs.onlinelibrary.wiley.com/doi/full/10.1002/2013RS005268

[12] D. D. Morabito, L. R. D'Addario, R. J. Acosta, and J. A. Nessel, "An Inter-Comparison of Two Independent Site Test Interferometers Located in Goldstone, California: Initial Study Results," *Proceedings of the 18th Ka and Broadband Communications, Navigation and Earth Observation Conference,* Ottawa, Canada, September 2012.

[13] D. D. Morabito, L. R. D'Addario, S. Keihm, and S. Shambayati, "Comparison of Dual Water Vapor Radiometer Differenced Path Delay Fluctuations and Site Test Interferometer Phase Delay Fluctuations Over a Shared 250-Meter Baseline," *The Interplanetary Network Progress Report,* vol. 42-188, Jet Propulsion Laboratory, Pasadena, California, pp. 1–21, February 15, 2012. https://ipnpr.jpl.nasa.gov/progress_report/42-188/188A.pdf

[14] D. D. Morabito, L. R. D'Addario, and S. Finley, "A Comparison of Atmospheric Effects on Differential Phase for a Two-Element Antenna Array and Nearby Site Test Interferometer," *Radio Science,* vol. 51, no. 2, pp. 91–103, February 2016. doi:10.1002/2015RS005763. https://agupubs.onlinelibrary.wiley.com/doi/10.1002/2015RS005763

[15] D. D. Morabito, L. R. D'Addario, and S. Finley, "Comparison of Atmospheric Delay Statistics from Deep Space Network Arrays and nearby Site Test Interferometers," *Proceedings of 22nd Ka- and Broadband Conference,* Cleveland, Ohio, October 17–20, 2016.

[16] D. D. Morabito and L. R. D'Addario, "Atmospheric Array Loss Statistics for the Goldstone and Canberra DSN Sites Derived from Site Test Interferometer Data," *The Interplanetary Network Progress Report,* vol. 42-196, Jet Propulsion Laboratory, Pasadena, California, pp. 1–23, February 15, 2014. https://ipnpr.jpl.nasa.gov/progress_report/42-196/196A.pdf

[17] D. D. Morabito and L. R. D'Addario, "Two-Element Uplink Array Loss Statistics Derived from Site Test Interferometer Phase Data for the Goldstone Climate: Initial Study Results," *The Interplanetary Network Progress Report,* vol. 42-186, Jet Propulsion Laboratory, Pasadena, California, pp. 1–20, August 15, 2011. https://ipnpr.jpl.nasa.gov/progress_report/42-186/186B.pdf

[18] D. D. Morabito and L. R. D'Addario, "Atmospheric Array Loss Statistics Derived from Short Time Scale Site Test Interferometer Phase Data," *The Interplanetary Network Progress Report,* vol. 42-198, Jet Propulsion Laboratory, Pasadena, California, pp. 1–20, August 15, 2014. https://ipnpr.jpl.nasa.gov/progress_report/42-198/198C.pdf

[19] L. R. D'Addario, "Combining Loss of a Transmitting Array Due to Phase Errors," *The Interplanetary Network Progress Report,* vol. 42-175, Jet Propulsion Laboratory, Pasadena, California, pp. 1–7, November 15, 2008. https://ipnpr.jpl.nasa.gov/progress_report/42-175/175G.pdf

[20] D. D. Morabito and J. Nessel, "Contributions to the Propagation Databanks: Path Length Turbulence Statistics for Goldstone, CA (Apollo Site); Canberra, AUST; Madrid, Spain; and Kennedy Space Center, Florida," *U.S. Radiocommunication Sector Fact Sheet,* ITU Document USWP 3M-5, January 27, 2017.

[21] D. D. Morabito and J. Nessel, "Application, Validation and Data Processing of Atmospheric Path Length Standard Deviation Statistics for Ground-based Antenna Array Performance Predictions," *U.S. Radiocommunication Sector Fact Sheet,* ITU-R Document USWP 3M-9, January 18, 2017.